Altered Mitochondrial Dynamics Contributes to Propofol-Induced Cell Death in Human Stem Cell-Derived Neurons

Danielle M. Twaroski, Ph.D.[*], **Yasheng Yan, B.S.**[#], **Ivan Zaja, M.D.**[*], **Eric Clark, B.S.**[‡], **Zeljko J. Bosnjak, Ph.D.**[§], and **Xiaowen Bai, M.D., Ph.D.**[†]

[*]Post-Doctoral Fellow, Departments of Physiology and Anesthesiology, Medical College of Wisconsin, Milwaukee, Wisconsin

[#]Research Associate, Department of Anesthesiology, Medical College of Wisconsin, Milwaukee, Wisconsin

[‡]Graduate Student, Department of Neuroscience, Medical College of Wisconsin, Milwaukee, Wisconsin

[§]Professor, Departments of Physiology and Anesthesiology, Medical College of Wisconsin, Milwaukee, Wisconsin

[†]Associate Professor, Departments of Physiology and Anesthesiology, Medical College of Wisconsin, Milwaukee, Wisconsin

Abstract

Background—Studies in developing animals have shown that when anesthetic agents are administered early in life, it can lead to neuronal cell death and learning disabilities. Development of human embryonic stem cell (hESC)-derived neurons has provided a valuable tool for understanding the effects of anesthetics on developing human neurons. Unbalanced mitochondrial fusion/fission leads to various pathological conditions including neurodegeneration. The aim of this study was to dissect the role of mitochondrial dynamics in propofol-induced neurotoxicity.

Methods—TUNEL staining was used to assess cell death in hESC-derived neurons. Mitochondrial fission was assessed using TOM20 staining and electron microscopy. Expression of mitochondrial fission-related proteins was assessed by Western blot and confocal microscopy was used to assess opening time of the mitochondrial permeability transition pore (mPTP).

Results—Exposure to 6 hours of 20 μg/mL propofol increased cell death from $3.18\pm0.17\%$ in the control-treated group to $9.6\pm0.95\%$ and led to detrimental increases in mitochondrial fission (n=5 coverslips/group) accompanied by increased expression of activated dynamin-related protein 1 (Drp1) and cyclin-dependent kinase 1 (CDK1), key proteins responsible for mitochondrial fission. Propofol exposure also induced earlier opening of the mPTP from 118.9 ± 3.1 seconds in the control-treated group to 73.3 ± 1.6 seconds. Pretreatment of the cells with mdivi-1, a mitochondrial

---

Address correspondence to: Xiaowen Bai, MD, PhD, Department of Anesthesiology, Medical College of Wisconsin, 8701 Watertown Plank Road, Milwaukee, Wisconsin 53226. xibai@mcw.edu. Phone: (414) 955-5755 and fax: (414) 955-6122).

fission blocker rescued the propofol-induced toxicity, mitochondrial fission and mPTP opening time (n=75 cells/group). Inhibiting CDK1 attenuated the increase in cell death and fission and the increase in expression of activated Drp1.

Conclusions—These data demonstrate for the first time that propofol-induced neurotoxicity occurs through a mitochondrial fission/mPTP-mediated pathway.

Introduction

When administered early in life, anesthetics, including propofol can lead to death of the neurons and neuronal supporting cells and have been associated with increased risk of learning, memory and behavioral deficiencies.[1–6] These detrimental effects have been well-established in many animal models and have raised safety concerns regarding the use of anesthetics in children. While millions of children are exposed to anesthetics every year, the use of these anesthetics in imaging or surgery is undeniably necessary.[7] Despite the large scale efforts of research initiatives like SmartTots, an organization tasked with evaluating the safety of anesthetics on the developing human brain, the effects of anesthetics in children remains uncertain.[8–10]

The human epidemiological studies conducted thus far have produced widely variable results[11–13] and the discrepancy in the results of these studies highlights the importance of developing a better human model by which to study the effects of anesthetics on the immature human brain. Human embryonic stem cells (hESCs) are pluripotent cells that can replicate indefinitely and are capable of differentiating into any cell type.[14, 15] Generating neurons from hESCs provides us with an essentially endless supply of human cells by which to study the effects of anesthetics on developing human neurons and the mechanisms governing anesthetic-induced neurotoxicity.

The mitochondria of the cell are extremely important organelles involved in many cellular processes including energy production, cell signaling and apoptosis.[16] To maintain proper functioning, the mitochondria continuously undergo cycles of fusion and fission. Unbalanced fusion/fission can sometimes lead to various pathological conditions including neurodegeneration and has been linked to many neurodegenerative disorders.[17–21] Dynamin-related protein 1 (Drp1) is a key regulator of mitochondrial fission. Phosphorylation of Drp1 by cyclin-dependent kinase 1 (CDK1) at the Serine616 position induces mitochondrial fission.[22–24] Mitochondrial fusion is regulated primarily by the proteins mitofusion 1 and 2 (MFN1 and MFN2) and optic atrophy 1 (OPA1). Previous studies have shown that exposure of neonatal rat pups to general anesthetics induces significant increases in mitochondrial fission.[25, 26] However, the role of mitochondrial dynamics and related pathways in propofol-induced neurotoxicity has yet to be investigated.

The mitochondrial permeability transition pore (mPTP) is a pore that spans the outer and inner mitochondrial membranes and is opened by oxidative stress.[27] When the mPTP opens, there is a large influx of solutes and water into the mitochondria. This can lead to swelling and eventual rupture of the mitochondria and cell death.[28] Inhibition of mPTP opening has been shown to attenuate ethanol-induced neurotoxicity in mice.[29] However, the role of mPTP opening and its connection to mitochondrial fission in propofol-induced neurotoxicity

has yet to be studied. The aim of this study was to dissect the role of mitochondrial dynamics and mPTP opening in propofol-induced neurotoxicity. We hypothesized that propofol would induce hESC-derived neuronal cell death though CDK1-mediated activation of Drp1, increased mitochondrial fission and mPTP opening.

Materials and Methods

hESC Culture and Differentiation into Neurons

All human cell experiments described were approved by the Institutional Review Board at the Medical College of Wisconsin (Milwaukee, WI, USA). Human embryonic stem cells (H1 line, WiCell Research Institute Inc., Madison, WI) were cultured as previously described by our laboratory on a feeder layer of mitotically inactivated mouse embryonic fibroblasts (MEFs).[30–32] Briefly, hESCs were plated onto MEFs that had been cultured on matrigel-coated 60 mm dishes. The hESCs were cultured in hESC media consisting of DMEM/F12 supplemented with 20% Knockout serum (Life Technologies, Grand Island, NY, USA), 1% nonessential amino acids, 1 mM L-glutamine, 1% penicillin-streptomycin (Life Technologies), 4 ng/mL human recombinant basic fibroblast growth factor (bFGF, Life Technologies) and 0.1 mM β-mercaptoethanol (Sigma-Aldrich, St. Louis, MO, USA) in the hypoxic incubator. The cells were mechanically passaged when confluent and the media was changed daily. Cells at passages 55–70 were used in these studies.

A 4-step directed differentiation protocol was used to generate neurons from the hESCs as previously described by our laboratory.[30–32] Briefly, the hESCs were dissociated from the MEF cultures and the pellet of hESCs was resuspended in hESC media without bFGF and the cells were cultured in a normoxic incubator (20% O_2/5% CO2, 37°C) on ultra-low attachment 6-well plates (Corning Inc., Corning, NY). Embryoid bodies (EBs) were present in the cultures 1 day after digestion and the media was changed daily. Five days after dispase digestion, the cultures were switched to neural induction media consisting of DMEM/F12 supplemented with 1% N2 (Life Technologies), 1% nonessential amino acids, 1 mg/mL heparin (Sigma) and 5 ng/mL bFGF and the media was changed daily for an additional 4 days. The EBs were then plated down to 35 mm, matrigel-coated dishes. The media was changed every other day until rosette-like structures were present in the cultures (within 5 days of plating). The rosettes were manually selected using a pipette tip and transferred to new, matrigel-coated 35 mm dishes and cultured in neural expansion media containing DMEM/F12 supplemented with 2% B27 without vitamin A, 1% N2 (Life Technologies), 1% nonessential amino acids, 20 ng/mL bFGF and 1 mg/mL heparin. The neural stem cells (NSCs) present in the rosettes were passaged enzymatically every 5 days using Accutase (Innovative Cell Technologies, San Diego, CA). To generate neurons, NSCs were cultured in matrigel-coated dishes to about 95% confluency. Once confluent, the cultures were switched to neuron differentiation media. The media was changed every other day and neurons were used for these studies 2 weeks after initiation of differentiation media.

Immunofluorescence Staining and Confocal Microscopy

hESC-derived neurons were cultured on matrigel-coated glass coverslips in neuron differentiation media for 2 weeks. Immunostaining was performed as previously described

by our laboratory.[30–32] Briefly, cells were fixed for 30 minutes at room temperature in 4% paraformaldehyde, washed and incubated in 0.5% Triton X-100 (Sigma-Aldrich) in PBS for 15 minutes. The cells were then incubated for 20 minutes in 10% Donkey Serum (blocking agent) at room temperature and placed in the primary antibodies [rabbit anti-β-tubulin III (neuron specific marker), mouse anti-doublecortin (immature neuron marker) (Abcam, Cambridge, MA), mouse TRITC-conjugated phalloidin (F-actin marker, Millipore) or rabbit anti-TOM20 (translocase of outer mitochondrial membranes 20 kDa, Santa Cruz, Dallas, Texas)] overnight at 4°C. Where appropriate, following incubation in the primary antibody, the cells were washed and incubated overnight at 4°C with Alexa Fluor 488 or 594 donkey anti-mouse or rabbit immunoglobulin G secondary antibodies (Life Technologies). The cells were incubated for 15 minutes at room temperature in Hoechst 33342 (Life Technologies) to stain the cell nuclei. The coverslips were mounted onto glass slides using mounting media and imaged using a laser-scanning confocal microscope (Nikon Eclipse Ti-E, Nikon Inc., Melville, NY).

Propofol, Mdivi-1 and Roscovitine Exposure

Brain concentrations of propofol in humans during anesthesia are believed to range between 4 and 20 μg/mL.[33, 34] We reported previously that propofol induced cell death in hESC-derived neurons in a dose- and exposure number-dependent manner.[32] All experiments in this study were performed in 2-week-old hESC-derived neurons following a single exposure to 6 hours of 20 μg/mL research grade propofol. The propofol was prepared as a 40 mg/mL stock solution in dimethyl sulfoxide (DMSO, Sigma-Aldrich) and diluted to the working concentration in neurobasal media. An equal volume of DMSO was used as the vehicle control. The cells were cultured in matrigel-coated 60 mm culture dishes (500,000 cells/dish) or 12 mm coverslips (100,000 cells/coverslip) and all exposures were done in a humidified chamber at 37°C.

Mdivi-1 is a selective inhibitor of dynamin-related protein 1 (Drp1), a key protein responsible for inducing mitochondrial fission. We utilized mdivi-1 (Sigma-Aldrich) to understand the role of mitochondrial fission in propofol-induced neurotoxicity. hESC-derived neurons were pretreated for 1 hour with 25 μM mdivi-1 in a humidified, 37°C incubator. The cells were washed once with neurobasal media and immediately exposed to 6 hours of propofol or DMSO. A 50 mM stock solution of mdivi-1 was prepared in DMSO and diluted to the working concentration in neurobasal media. During the pretreatment period, control cells were exposed with an equal volume of DMSO ("mdivi-1 control") or neurobasal media alone ("no treatment" group). Following the propofol exposure, the cells were immediately fixed for TOM20 or TUNEL staining.

Roscovitine is a selective inhibitor of several cyclin-dependent kinases including CDK1. Roscovitine has been shown in both *in vivo* and *in vitro* models to reduce neuronal cell death and neurological deficits following brain trauma, cerebral ischemia and trophic deprivation.[35–37] However, the mechanism by which Roscovitine provides neuroprotection and the role of CDK1 inhibition in anesthetic-induced neurotoxicity has yet to be studied. hESC-derived neurons were pretreated for 1 hour with 10 μM Roscovitine (Sigma-Aldrich) at 37°C. The cells were washed with fresh neurobasal media and exposed for 6 hours to

propofol or DMSO. The stock solution of Roscovitine was prepared in DMSO and diluted in neurobasal media to the working concentration. To ensure that the DMSO was not producing an effect, the control cells were exposed during the pretreatment to either neurobasal media alone ("no treatment" group) or an equal volume of DMSO ("Roscovitine control" group).

TUNEL Staining

To assess cell death in the hESC-derived neurons, a cell death detection kit (Roche Applied Bio Sciences, Indianapolis, IN) was used following instructions provided by the manufacturer. This kit utilizes a process known as terminal deoxynucleotidyl transferase-mediated deoxyuridine triphosphate in situ nick end labeling (TUNEL) to label the free 3′-OH termini of single and double stranded DNA breaks. The polymerase, terminal deoxynucleotidyl transferase (TdT) adds modified nucleotides to the free 3′-OH termini which are secondarily labeled with a fluorescent marker. This allows for the visualization of TUNEL positive cells on a fluorescent microscope.

hESC-derived neurons were cultured on glass coverslips and exposed to propofol or DMSO with or without mdivi-1 pretreatment. The cells were rinsed with PBS following an 18 hour washout in fresh neurobasal media and fixed for 30 minutes with 4% PFA. Fragmented DNA was labeled using the TUNEL staining kit and the cells were stained for 15 minutes with Hoechst 33342 to label the cell nuclei. The coverslips were mounted to glass slides and imaged at 200x total magnification using a fluorescent microscope. A minimum of 5–6 images was taken per coverslip with each image containing around 100 cells. Therefore, approximately 500 cells were imaged for each coverslip and 5 coverslips were imaged per group. Cell death was quantified by manually counting the number of TUNEL positive cells in the field and the total cell nuclei. The data is expressed as a percent of TUNEL positive cells present in the field. For these experiments, the coverslips were placed in separate wells of a 24-well plate. To eliminate the possibility of bias introduced in the plate, the coverslips were assigned randomly to the different groups across the entire plate. In addition, the experimenter was blinded to the groups being imaged and analyzed to eliminate the possibility of bias introduced by the experimenter.

Mitochondrial Morphology Analysis

To assess changes in mitochondrial morphology, hESC-derived neurons were exposed to mdivi-1 and/or propofol or DMSO and fixed in 4% PFA. The cells were stained using the TOM20 primary antibody to label the mitochondria as described above in the "immunofluorescence staining" section. The cells were imaged using the confocal microscope and single cell images were captured. The images were analyzed using the ImageJ 1.47v software (Wayne Rasband, National Institutes of Health) as previously described by our laboratory.[30] Briefly, the fluorescent images were converted to binary images and the length, area, width and perimeter of the mitochondria were determined. To assess the mitochondrial morphology, the aspect ratio (AR) and form factor (FF) were calculated for each cell. The AR is a measure of the length of the mitochondria and is calculated as the ratio of the major to minor axes of the ellipse while the FF is a measure of the degree of mitochondrial branching and is calculated using the equation: FF =

perimeter^2/4π × area. The minimum value for both parameters is 1 which would represent a sphere. Healthy, elongated and interconnected mitochondria have a high FF and AR while fragmented, discontinuous mitochondria have low FF and AR values. For each group, 15 cells were imaged and analyzed from 5 coverslips (75 cells analyzed per group). The images from the 15 cells were averaged for each coverslip. The n is the number of coverslips imaged which is 5 for each group. To minimize bias introduced by the experimenters, one experimenter was responsible for exposing the cells to the various conditions and another experimenter (who was blinded to the groups being studied) was responsible for imaging and data analysis.

Electron Microscopy

hESC-derived neurons were cultured on matrigel-coated plastic coverslips and were exposed to propofol or DMSO with or without mdivi-1 pretreatment. The cells were immediately fixed at 4°C with 2% glutaraldehyde in 0.1M sodium cacodylate buffer and postfixed for 1 hour on ice with 1% osmium tetroxide. The cells were rinsed with distilled water and dehydrated using acetonitrile and graded methanol (50%, 20 minutes; 70%, 20 minutes; 95%, 20 minutes; 100% 3x, 20 minutes). The cells were embedded in epoxy resin (EMbed-812, Electron Microscopy Sciences, Hatfield, PA) and polymerized at 70°C overnight. Thin (60nm) sections were cut and the sections were stained with lead citrate and uranyl acetate. The samples were imaged using a Hitachi H600 Electron Microscope.

Mitochondrial Permeability Transition Pore (mPTP) Opening and Membrane Potential

NSCs were cultured on glass coverslips for 2 weeks in neuron differentiation media. The hESC-derived neurons were exposed to propofol/DMSO with or without mdivi-1 pretreatment as described. The cells were then loaded for 20 minutes at 37°C with Hoechst 33342 and 50 nM tetramethylrhodamine ethylester (TMRE, Life Technologies), a lipophilic, membrane potential-dependent fluorescent dye that is readily taken up by mitochondria. The cells were washed with fresh neurobasal media and imaged using a confocal microscope. Rapid laser scanning with the 561 nm emission line laser of the confocal microscope was used to induce oxidative stress and opening of the mPTP by exposing a single cell to laser excitation every 3.5 seconds for 55 frames. Opening of the mPTP was visualized as a rapid loss of TMRE fluorescence. The arbitrary mPTP opening time was assessed by determining the time when the TMRE fluorescence had decreased by half from the baseline TMRE fluorescence intensity to the residual TMRE fluorescence intensity. An earlier opening of the mPTP is indicative of increased vulnerability of the cells to stress. When analyzing the images, a small area of mitochondria (the size of which was held constant across groups and images) was analyzed. This was intended to prevent any change in mitochondrial number or surface area across groups from influencing the results since we were only interested in the time it took the pore to open. Neurons loaded with TMRE and Hoechst 33342 following propofol or DMSO exposure were also imaged on the confocal microscope to assess the mitochondrial membrane potential. The fluorescence intensity of each cell (area of analysis held constant across groups) was measured using the ImageJ software and the mitochondrial membrane potential was reported in arbitrary units. To minimize any potential bias in the results, the experimenter was blinded to the group being imaged and analyzed.

Western Blot

hESC-derived neurons were exposed to Propofol or DMSO with or without mdivi-1 pretreatment, rinsed with PBS and immediately lysed in RIPA lysis buffer (Cell Signaling, Danvers, MA) containing phosphatase inhibitor cocktail (Roche Diagnostics) as described previously by our laboratory.[32] Total protein concentration was determined for each sample and the samples were boiled for 5 min at 97°C. Following the denaturation step, 25μg of protein/lane was loaded to gels for SDS-PAGE separation. Following the gel separation, the protein was transferred to a nitrocellulose membrane and the membranes were blocked. The membranes were then incubated at 4°C overnight with the primary antibodies: rabbit anti-phosphorylated Drp1 (pDrp1 Ser 616) (Cell Signaling, Danvers, MA), mouse anti-Drp1 (BD Technologies, Durham, NC), mouse anti-CDK1 (Santa Cruz), rabbit anti-OPA1, mouse anti-Mitofusion 1 or mouse anti-Mitofusion 2 (Abcam). The membranes were then incubated for 1 hour at room temperature with secondary antibodies conjugated to horseradish peroxidase (Cell Signaling). The antibody labeled proteins were then detected with chemiluminescence detection reagent (Cell Signaling) and exposed on x-ray film. To quantify the optical densities from the x-ray films, the ImageJ software was used. For all Western blots, an n of 5 was used which represents 5 Western blots run from 5 separate preparations with each preparation containing 5 60 mm culture dishes of neurons for each group run.

Statistical Analysis

All experiments were performed on samples from 3–4 independent neuronal differentiations. We chose to use a sample size of n = 5 coverslips/dishes for our experiments. This was based on previous findings by our group indicating that an n of 3 is sufficient in this model, but an n of 5 provides greater confidence in the results generated. The sample size was increased during the review process, but no adjustments were made for multiple comparisons. Values had normal distributions and were reported at mean ± SEM. When 2 groups were compared, a Student's t-test was used and one way analysis of variance (ANOVA) with a Tukey correction for multiple testing was used when more than 2 groups were compared. The SigmaPlot 12.5 software (Systat Software, Inc., San Jose, CA) was used for all statistical analysis and a two-tailed P-value < 0.05 was considered significant.

Results

Characterization of human embryonic stem cell (hESC)-Derived Neurons and Propofol-Induced Cell Death

hESCs were taken through a 4-step differentiation protocol using chemically defined media to generate neurons. The cells were characterized using immunofluorescence staining following 2 weeks in differentiation media. About 90–95% of the cells in culture stained positive for the neuron-specific marker, β-tubulin III (fig. 1A–a), indicating that the differentiation protocol was highly efficient in the generation of neurons. The cells also displayed a morphology characteristic of neurons with small cell bodies and long, interrelating projections. Although this immunostaining confirmed the purity of the cultures, it did not establish the maturity level of the cells. To assess the maturity level of the generated neurons, the cells were immunostained using the doublecortin antibody, a marker of migratory and immature neurons. Most of the neurons generated (90–95%) stained

positive for this marker of immature neurons (fig. 1A–b). In addition, the β-tubulin III and doublecortin staining co-localized (fig. 1A–c). Our laboratory has shown previously that these cultures display synapse-like structures and express additional neuronal markers as well as pre- and post-synaptic markers.[30–32]

We have shown previously that propofol induced cell death in hESC-derived neurons in a dose and exposure number-dependent manner.[32] Exposure to 6 hours of 20 μg/mL propofol induced a significant increase in TUNEL positive cells when compared to vehicle/control (DMSO)-treated cells, indicating a significant increase in cell death (fig. 1B). In the control treated group, $3.18 \pm 0.17\%$ of the cells were TUNEL positive while $9.6 \pm 0.95\%$ of the cells were TUNEL positive in the propofol treated group. The cells were exposed to 6 hours of 10 μg/mL propofol, 20 μg/mL propofol or the vehicle control then co-stained for the neuron-specific marker, β-tubulin III and phalloidin, an F-actin marker. Nearly all of the cells in culture in all groups stained positive for the neuron specific marker, indicating high differentiation efficiency (fig. 1C). Following exposure to 10 μg/mL propofol, the actin cytoskeleton of the β-tubulin III stained neurons appeared disorganized when compared to control-treated cells as assessed by phalloidin staining. The cytoskeletal disruption was further exacerbated in the 20 μg/mL propofol-treated group (fig. 1D). This data ultimately suggests that the propofol-induced mitochondrial fission is detrimental to the formation of the neuronal network and cytoskeletal disorganization has been linked to apoptosis.[38–40]

Propofol Exposure Increases Mitochondrial Fragmentation

To assess changes in mitochondrial dynamics (mitochondrial fusion and fission), hESC-derived neurons were exposed to propofol or the vehicle control for 6 hours and immunostained for TOM20. The cells were exposed to 0, 5, 10 and 20 μg/mL propofol and imaged on the confocal microscope using a 488 nm laser to visualize the mitochondria. There was a dose-response to propofol of mitochondrial fission in the cells. In control-treated cells and 5 μg/mL propofol treated cells, the mitochondria appeared elongated and interconnected. In contrast, the mitochondria appeared visibly smaller in the 10 μg/mL propofol-treated group and severely fragmented and discontinuous in the 20 μg/mL propofol-treated group. These results were quantified by assessing the FF and AR of the cells and both measurements were reduced in the 10 μg/mL propofol-treated group with a greater reduction in the 20 μg/mL propofol-treated group (fig. 2). Cells were then exposed to 6 hours of 20 μg/mL propofol or the vehicle control following a 1 hour pretreatment with mdivi-1 or control (DMSO) and immunostained for TOM20. The mitochondrial in the control-treated groups appeared healthy and elongated. The mitochondria were severely fragmented in the groups treated with propofol following pretreatment for 1 hour with media alone (no treatment) or the mdivi-1 control. The mitochondrial morphology appeared to return to control conditions in cells pretreated with mdivi-1 prior to the propofol exposure (fig. 3A a).

To quantify the changes in mitochondrial morphology, ImageJ software was used to analyze the confocal images. Following exposure to propofol, the cells had significantly lower AR and FF values compared to control treated cells indicating that the mitochondria were significantly shorter and less branched, respectively (fig. 3A b–c). The AR and FF of the

control treated cells were 4.11 ± 0.15 and 6.35 ± 0.38, respectively. In propofol-treated cells, the AR and FF were reduced to 2.27 ± 0.09 and 3.04 ± 0.06, respectively, indicating significant mitochondrial fission. The mitochondrial fission in the propofol-treated group was not rescued by pretreatment of the cells with the mdivi-1 control (AR: 2.49 ± 0.15, FF: 3.16 ± 0.09), but was rescued to control values when the cells were pretreated with 25 μM of the mitochondrial fission blocker, mdivi-1 (AR: 4.72 ± 0.18, FF: 6.85 ± 0.31).

To further assess changes in mitochondrial morphology, the cellular ultrastructure of hESC-derived neurons exposed to propofol or the vehicle control was imaged using an electron microscope. In the control-treated group, the mitochondria appeared elongated and branched with a long oval appearance and regular cristae. In contrast, when the cells were treated with propofol, the mitochondria became strikingly smaller and more spherical in shape. When the cells were pretreated for 1 hour with 25 μM mdivi-1 prior to the propofol exposure, the cellular ultrastructure returned to control conditions with the mitochondria appearing elongated and healthy (fig. 3B).

Propofol-Induced Cell Death is Attenuated by Pretreatment of the Cells with Mdivi-1

TUNEL staining was used to assess cell death in hESC-derived neurons following exposure to propofol or the vehicle control with or without mdivi-1 pretreatment. The number of TUNEL-positive cells appeared considerably higher in the propofol-treated group when compared to the control-treated groups (fig. 4A). To quantify the results, the cells were manually counted to obtain a percent of TUNEL-positive cells. Once again, propofol induced a significant increase in TUNEL-positive cells ($7.54 \pm 0.2\%$) when compared to control treated cells ($1.81 \pm 0.37\%$). The increase in TUNEL-positive cells was partially attenuated by pretreatment of the cells for 1 hour with 25 μM of the mitochondrial fission blocker, mdivi-1 ($3.02 \pm 0.23\%$) prior to propofol exposure, suggesting that mitochondrial fission plays an important role in propofol-induced cell death (fig. 4B).

Exposure of hESC-Derived Neurons to Propofol Induces Alterations in the Expression of Mitochondrial Fission-Related Proteins

To further dissect the mechanism of propofol-induced neurotoxicity in hESC-derived neurons, the expression of key mitochondrial fission and fusion related proteins was assessed by Western blot (fig. 4). We found that the level of activated Drp1 (pDrp1 Ser 616), a protein important in inducing mitochondrial fission, was significantly increased following propofol exposure (fig. 5A), confirming propofol-induced increases in mitochondrial fission through Drp1 activation. However, there was no significant change in the expression of any of the mitochondrial fusion-related proteins (MFN1, MFN2 or OPA1) following propofol exposure, suggesting that propofol alters mitochondrial dynamics through effects only on mitochondrial fission (fig. 5B).

Cyclin-Dependent Kinase 1 (CDK1) Inhibition Attenuates Propofol-Induced Cell Death, Drp1 Activation and Mitochondrial Fission

CDK1 is a kinase and has been reported to be involved in phosphorylation and activation of Drp1.[24, 41] The expression of CDK1 was increased following exposure to propofol as assessed by Western blot (fig. 6A). Inhibition of CDK1 with the chemical blocker

Roscovitine attenuated the propofol-induced cell death as assessed by TUNEL staining (Fig. 6B). Additionally, pretreatment of the cells with Roscovitine reduced the expression of pDrp1 (Ser616) (fig. 6C), suggesting that the propofol-induced increase in CDK1 expression is inducing mitochondrial fission and cell death through activation of Drp1. Pretreatment of the cells with Roscovitine also attenuated the propofol-induced mitochondrial fission, further confirming a role for CDK1 in the mechanism of propofol-induced neurotoxicity (fig. 6D).

Propofol Exposure Reduces the Mitochondrial Membrane Potential and Induces an Earlier Opening of the Mitochondrial Permeability Transition Pore (mPTP)

To assess the downstream pathway of propofol-induced neuronal cell death, mPTP opening time was analyzed. hESC-derived neurons were loaded with TMRE, a cationic dye that is readily sequestered by the mitochondria. The mitochondria appeared elongated and healthy in all control-treated groups, but appeared severely fragmented in the propofol treated group on confocal microscopy images. Once again, the mitochondria appeared healthy in the propofol group when the cells were pretreated with mdivi-1 (fig. 7A). Opening of the mPTP was then induced using rapid laser scanning on the confocal microscope. The arbitrary mPTP opening time was calculated as the time at which the TMRE fluorescence intensity had decreased by half. Figure 7B depicts the quantified mPTP opening times for each group. The mPTP opened earlier in the propofol no treatment and propofol mdivi-1 control treated groups when compared to all other groups, suggesting that mPTP opening is likely involved in the mechanism governing propofol-induced cell death. In addition, the mPTP opening was rescued by pretreatment of the cells with mdivi-1, suggesting an important connection between mitochondrial fission and mPTP opening. Decreased mitochondrial membrane potential has been reported to be related to matrix configuration and cytochrome c release during apoptosis.[42] Exposure to 6 hours of 20 μg/mL propofol induced a significant decrease in the mitochondrial membrane potential of the hESC-derived neurons, further indicating mitochondrial damage (fig. 7C).

Discussion

In this study, changes in mitochondrial dynamics following propofol exposure in hESC-derived neurons and the role that these changes play in propofol-induced neurotoxicity were assessed. Exposure of hESC-derived neurons to 20 μg/mL propofol for 6 hours induced significant cell death, increased mitochondrial fission and led to earlier opening of the mPTP and a decrease in the mitochondrial membrane potential. Additionally, we showed that propofol altered the expression of CDK1 and Drp1, key proteins involved in mitochondrial fission, but did not significantly alter the expression of mitochondrial fusion-related proteins. Collectively, our data indicates, for the first time, that propofol induces neuronal cell death through CDK1/Drp1-induced mitochondrial fission and mPTP opening.

The developing brain is most vulnerable to anesthetic exposure during the period of rapid synaptogenesis, which in humans ranges from the third trimester of pregnancy through the third year of life.[43] It is difficult to accurately assess the maturity level of hESC-derived neurons due to a lack of information regarding neuronal characteristics during human brain

development. However, most of the hESC-derived neurons in our cultures stained positive for doublecortin, a marker of immature neurons (fig. 1A). Although it is not possible to determine the exact developmental stage of the stem cell-derived neurons, they are immature and vulnerable to anesthetic-induced cell death. Our laboratory showed previously that these cells also express the pre- and post-synaptic markers, Synapsin I and Homer I, respectively and display synapse-like structures upon electron microscopy imaging, indicating that they also form synapses in culture.[30, 32] Therefore, we have developed a culture system of pure, immature and functional neurons which allows us to study the mechanisms governing propofol-induced neurotoxicity in a human model. The mechanisms by which anesthetics induce neurotoxicity remain largely unknown. MicroRNAs, neuroinflammation, calcium signaling and reactive oxygen species production all appear to play a role in the toxicity.[30, 32, 44–46] In this study, we examined the role of mitochondrial dynamics in the mechanism of propofol-induced neurotoxicity.

In this study, we found that exposure of hESC-derived neurons to 6 hours of 20 μg/mL propofol induced significant cell death and disorganization of the actin cytoskeleton (fig. 1B, C, D). Increases in mitochondrial fission have been shown to induce apoptosis- and necrosis-mediated cell death in some studies.[47, 48] Additional studies have demonstrated that inhibition of Drp1 could prevent increases in mitochondrial fission and lead to increased neuronal cell survival, implicating Drp1 inhibition as a potential neuroprotective strategy.[49] It is important to note that the process of mitochondrial fusion and fission is extremely complex and increases in mitochondrial fission have been shown to be beneficial in certain cell types.[50] However, the role of mitochondrial fission in anesthetic-induced cell death is just beginning to be understood. It has been shown that exposure to a combination of general anesthetics for 6 hours in 7-day old rat pups induced significant mitochondrial fission.[25] Additionally, our lab has shown previously that exposure of hESC-derived neurons to 24 hours of 100μM ketamine induced an increase in cell death and mitochondrial fission.[30] However, the functional role of mitochondrial dynamics in anesthetic-induced neurotoxicity has yet to be studied. In this study, propofol dose-dependently induced mitochondrial fission in the hESC-derived neurons. The propofol-mediated increase in mitochondrial fission and cell death could be prevented by pretreatment of the cells with the mitochondrial fission blocker, mdivi-1 (fig. 3 and 4). This suggests that mitochondrial fission is involved in propofol-induced neurotoxicity. However, pretreatment of the cells with mdivi-1 did not return the propofol-induced cell death all the way back to control levels. This highlights the complexity of the mechanisms governing propofol-induced neurotoxicity. Although the pathway we have elucidated in this study does appear to play an important role in this process, the role of additional pathways cannot be excluded.

To understand the upstream effectors of mitochondrial fission following propofol exposure, we began by looking at the expression of Drp1. Drp1 is an important protein responsible for inducing mitochondrial fission and it has been shown in primary cortical rat cultured neurons that recruitment of Drp1 along with several proteins plays a role in mitochondrial fission and cell death under excitotoxic conditions.[51] Drp1 is activated primarily by phosphorylation at the Serine 616 position.[48] We found that the expression of activated Drp1 was substantially increased following exposure to propofol (fig. 5). Drp1 is phosphorylated at the Ser616 position and activated predominantly by CDK1.[22] Taguchi and

colleagues were the first to report that CDK1 is responsible for phosphorylating and activating Drp1 in rat cultures at the Serine 585 position, which is equivalent in humans to the Serine 616 position.[52] They went on to show that activation of Drp1 by CDK1 leads to increased mitochondrial fission. More recently, it was shown by immunoprecipitation that CDK1 and Drp1 interact in cultured mouse cardiomyocytes and that blockade of CDK1 with Roscovitine in these same cells decreases the expression of pDrp1 Serine 616.[53] Drp1 regulation is complex and involves many additional proteins. For example, phosphorylation of Drp1 at the Serine 637 position by protein kinase A leads to inactivation of Drp1 and a decrease in mitochondrial fission while dephosphorylation of Drp1 at the same position by calcineurin results in activation of Drp1.[54] CDK1 remains a key protein in Drp1 activation and mitochondrial fission. It has been shown that pretreatment of primary neuron cultures with various CDK1 inhibitors can protect against neuronal cell death.[35] We found that the expression of CDK1 was increased in the hESC-derived neurons following exposure to propofol (fig. 6A). Finally, we found that pretreatment of the cells with the CDK1 blocker, Roscovitine could rescue the propofol-induced cell death, activation of Drp1 and increase in mitochondrial fission, further suggesting a functional role of CDK1 in propofol-induced neurotoxicity. Nevertheless, mitochondrial fission and Drp1 activation are extremely complex and as such, the potential role of additional unstudied components cannot be excluded.

To understand the downstream components of the propofol-induced mitochondrial fission pathway, we evaluated changes in mPTP opening time. Several studies have implicated mitochondrial fission, opening of the mPTP and loss of the mitochondrial membrane potential as a key cascade of events that leads to cell death following a stress.[55, 56] Mitochondrial fission has been shown to induce earlier opening of the mPTP, and mPTP opening induces cell death.[22, 56] Blockade of mPTP opening has been shown to attenuate ethanol-induced neurotoxicity. *In vitro* cultures of primary mouse neurons and astrocytes and 7-day-old mouse pups were exposed to multiple doses of ethanol. Ethanol exposure induced mPTP opening and cell death in the cultures and widespread neuronal cell death and behavioral abnormalities *in vivo*. The cell death and behavioral changes were attenuated by blockade of mPTP opening.[57] This was of interest since ethanol and propofol both act on the GABA$_A$ receptor in the brain. The role of mPTP opening and the link between mitochondrial fission and the mPTP has yet to be studied in anesthetic-induced neurotoxicity. We found that the mPTP opened earlier in cells treated with propofol or the mdivi-1 control when compared to all control-treated groups. Opening of the mPTP was delayed in cells pretreated with mdivi-1, suggesting that increases in mitochondrial fission induced by propofol might lead to mPTP opening and, ultimately, cell death (fig. 7A, B).

Although the culture of human neurons from stem cells is a useful and promising model for the study of neurotoxicity, the direct applicability of this data to developmental neurotoxicity in humans remains to be defined. This study alone cannot adequately address the role of mitochondrial abnormalities in propofol-induced neurotoxicity. Thus, future animal studies will be important to further assess the role of mitochondrial fission in propofol-induced neuronal death and cognitive deficits. In addition, the underlying mechanisms of anesthetic-induced developmental neurotoxicity are complex. Cell death

may not be the only determinate of later neurocognitive deficits. Other mechanisms such as abnormal neurogenesis and synaptogenesis might also contribute to the cognitive dysfunction. In the current study, we observed disorganization of the actin cytoskeleton at the lower, more clinically relevant dose of 10 μg/mL propofol (fig. 1C, D), suggesting that cellular abnormalities occur without cell death. The actin cytoskeleton can regulate many important cellular processes in the brain, including cell division, migration, cytokinesis, and differentiation.[58, 59] The potential contribution of disorganization of the actin cytoskeleton in propofol-induced developmental neurotoxicity will be explored in future studies.

One limitation of this study is that our *in vitro* model system contains only neurons. This is not truly representative of the human brain which is composed of neurons and several types of glial cells. Interactions between neurons and glial cells may alter the signaling pathways we have identified in this study as well as the responsiveness of neurons to propofol. Nevertheless it is critical to first understand the direct effects of propofol on human neurons, the mechanisms governing propofol-induced neuronal cell death and possible protective approaches before understanding how glial cells may alter these effects and pathways. Another limitation of this study is that the use of an *in vitro* culture system limits the data that can be obtained when compared to the use of an *in vivo* animal model. Cultured neurons lack stimuli from the complex network of cells that is found *in vivo* and endpoints of interest such as cognitive functioning cannot be assessed. However, this human model allows us to carefully dissect out mechanisms of anesthetic-induced developmental neurotoxicity that can potentially be translated to an animal model to further develop protective strategies against anesthetic-induced developmental neurotoxicity.

An additional limitation of this study is the supra-therapeutic dose of propofol used. Propofol is highly lipophilic and concentrates in lipid-rich tissues such as the brain.[60] It is uncertain what concentration of propofol neurons in the developing human brain are exposed to during surgery. In addition, many animal and human epidemiologic studies have shown that anesthetic-induced neurotoxicity is dose, time and exposure number dependent. This study focused on a single exposure to propofol with cell death used as the endpoint of interest. We have shown in the hESC-derived neurons that propofol induces cell death at lower doses following multiple exposures.[32] However, it is difficult to study the mechanisms by which this occurs when multiple exposures are involved. The high dose of propofol used in this study may limit how this data connects to the clinic. However, the results of this study may still be translatable to the human brain in which the same mechanisms could induce toxicity at different doses due to the increased vulnerability in the whole brain. Future studies aimed at understanding the role of mitochondrial abnormalities and the neurotoxic effects of propofol at lower doses by co-culturing hESC-derived neurons with glial cells and evaluating the effects of multiple exposures will be extremely important.

In conclusion, this study has established, for the first time, a role for mitochondrial fission and mPTP opening in propofol-induced toxicity in human neurons. These data suggest that propofol exposure in hESC-derived neurons leads to activation of Drp1 through CDK1, increases in mitochondrial fission, a decrease in the mitochondrial membrane potential and mPTP opening which, together induces cell death. The detrimental effects of anesthetics on the developing brain have been well-studied in animals. However, the mechanisms by which

these anesthetics induce toxicity remain unclear. Our *in vitro* human model of hESC-derived neurons has allowed us to study the mechanism by which propofol induces cell death. Nevertheless, future studies confirming these results in whole animal models will be important. Understanding the mechanisms by which propofol and other anesthetics induce toxicity in the developing brain is critical in order to develop potential protective strategies. The results of this study may one day contribute to the development of such approaches aimed at mitigating the neurotoxic effects of propofol in young children.

Acknowledgments

References

1. Anderson CM, Norquist BA, Vesce S, Nicholls DG, Soine WH, Duan S, Swanson RA. Barbiturates induce mitochondrial depolarization and potentiate excitotoxic neuronal death. The Journal of neuroscience : the official journal of the Society for Neuroscience. 2002; 22:9203–9. [PubMed: 12417645]

2. Brambrink AM, Back SA, Riddle A, Gong X, Moravec MD, Dissen GA, Creeley CE, Dikranian KT, Olney JW. Isoflurane-induced apoptosis of oligodendrocytes in the neonatal primate brain. Annals of neurology. 2012; 72:525–35. [PubMed: 23109147]

3. Creeley C, Dikranian K, Dissen G, Martin L, Olney J, Brambrink A. Propofol-induced apoptosis of neurones and oligodendrocytes in fetal and neonatal rhesus macaque brain. British journal of anaesthesia. 2013; 110(Suppl 1):i29–38. [PubMed: 23722059]

4. Jevtovic-Todorovic V, Hartman RE, Izumi Y, Benshoff ND, Dikranian K, Zorumski CF, Olney JW, Wozniak DF. Early exposure to common anesthetic agents causes widespread neurodegeneration in the developing rat brain and persistent learning deficits. The Journal of neuroscience : the official journal of the Society for Neuroscience. 2003; 23:876–82. [PubMed: 12574416]

5. Paule MG, Li M, Allen RR, Liu F, Zou X, Hotchkiss C, Hanig JP, Patterson TA, Slikker W Jr, Wang C. Ketamine anesthesia during the first week of life can cause long-lasting cognitive deficits in rhesus monkeys. Neurotoxicology and teratology. 2011; 33:220–30. [PubMed: 21241795]

6. Shen X, Liu Y, Xu S, Zhao Q, Guo X, Shen R, Wang F. Early life exposure to sevoflurane impairs adulthood spatial memory in the rat. Neurotoxicology. 2013; 39:45–56. [PubMed: 23994303]

7. Loepke AW, Soriano SG. An assessment of the effects of general anesthetics on developing brain structure and neurocognitive function. Anesthesia and analgesia. 2008; 106:1681–707. [PubMed: 18499597]

8. Miller TL, Park R, Sun LS. Report of the third PANDA symposium on "Anesthesia and Neurodevelopment in Children". Journal of neurosurgical anesthesiology. 2012; 24:357–61. [PubMed: 23076223]

9. Sun LS, Li G, DiMaggio CJ, Byrne MW, Ing C, Miller TL, Bellinger DC, Han S, McGowan FX. Feasibility and pilot study of the Pediatric Anesthesia NeuroDevelopment Assessment (PANDA) project. Journal of neurosurgical anesthesiology. 2012; 24:382–8. [PubMed: 23076226]

10. Sprung J, Flick RP, Katusic SK, Colligan RC, Barbaresi WJ, Bojanic K, Welch TL, Olson MD, Hanson AC, Schroeder DR, Wilder RT, Warner DO. Attention-deficit/hyperactivity disorder after early exposure to procedures requiring general anesthesia. Mayo Clinic proceedings. 2012; 87:120–9. [PubMed: 22305025]

11. Wilder RT, Flick RP, Sprung J, Katusic SK, Barbaresi WJ, Mickelson C, Gleich SJ, Schroeder DR, Weaver AL, Warner DO. Early exposure to anesthesia and learning disabilities in a population-based birth cohort. Anesthesiology. 2009; 110:796–804. [PubMed: 19293700]

12. Hansen TG, Pedersen JK, Henneberg SW, Pedersen DA, Murray JC, Morton NS, Christensen K. Academic performance in adolescence after inguinal hernia repair in infancy: a nationwide cohort study. Anesthesiology. 2011; 114:1076–85. [PubMed: 21368654]

13. Bartels M, Althoff RR, Boomsma DI. Anesthesia and cognitive performance in children: no evidence for a causal relationship. Twin research and human genetics : the official journal of the International Society for Twin Studies. 2009; 12:246–53. [PubMed: 19456216]

14. Coopman K. Large-scale compatible methods for the preservation of human embryonic stem cells: current perspectives. Biotechnology progress. 2011; 27:1511–21. [PubMed: 22235484]

15. Thomson JA, Itskovitz-Eldor J, Shapiro SS, Waknitz MA, Swiergiel JJ, Marshall VS, Jones JM. Embryonic stem cell lines derived from human blastocysts. Science. 1998; 282:1145–7. [PubMed: 9804556]

16. McBride HM, Neuspiel M, Wasiak S. Mitochondria: more than just a powerhouse. Current biology : CB. 2006; 16:R551–60. [PubMed: 16860735]

17. Knott AB, Bossy-Wetzel E. Impairing the mitochondrial fission and fusion balance: a new mechanism of neurodegeneration. Annals of the New York Academy of Sciences. 2008; 1147:283–92. [PubMed: 19076450]

18. Perfettini JL, Roumier T, Kroemer G. Mitochondrial fusion and fission in the control of apoptosis. Trends in cell biology. 2005; 15:179–83. [PubMed: 15817372]

19. Youle RJ, Karbowski M. Mitochondrial fission in apoptosis. Nature reviews Molecular cell biology. 2005; 6:657–63. [PubMed: 16025099]

20. Batlevi Y, La Spada AR. Mitochondrial autophagy in neural function, neurodegenerative disease, neuron cell death, and aging. Neurobiology of disease. 2011; 43:46–51. [PubMed: 20887789]

21. Burte F, Carelli V, Chinnery PF, Yu-Wai-Man P. Disturbed mitochondrial dynamics and neurodegenerative disorders. Nature reviews Neurology. 2015; 11:11–24. [PubMed: 25486875]

22. Cereghetti GM, Stangherlin A, Martins de Brito O, Chang CR, Blackstone C, Bernardi P, Scorrano L. Dephosphorylation by calcineurin regulates translocation of Drp1 to mitochondria. Proceedings of the National Academy of Sciences of the United States of America. 2008; 105:15803–8. [PubMed: 18838687]

23. Zhao J, Liu T, Jin S, Wang X, Qu M, Uhlen P, Tomilin N, Shupliakov O, Lendahl U, Nister M. Human MIEF1 recruits Drp1 to mitochondrial outer membranes and promotes mitochondrial fusion rather than fission. The EMBO journal. 2011; 30:2762–78. [PubMed: 21701560]

24. Bossy B, Petrilli A, Klinglmayr E, Chen J, Lutz-Meindl U, Knott AB, Masliah E, Schwarzenbacher R, Bossy-Wetzel E. S-Nitrosylation of DRP1 does not affect enzymatic activity and is not specific to Alzheimer's disease. Journal of Alzheimer's disease : JAD. 2010; 20(Suppl 2):S513–26. [PubMed: 20463395]

25. Boscolo A, Milanovic D, Starr JA, Sanchez V, Oklopcic A, Moy L, Ori CC, Erisir A, Jevtovic-Todorovic V. Early exposure to general anesthesia disturbs mitochondrial fission and fusion in the developing rat brain. Anesthesiology. 2013; 118:1086–97. [PubMed: 23411726]

26. Boscolo A, Starr JA, Sanchez V, Lunardi N, DiGruccio MR, Ori C, Erisir A, Trimmer P, Bennett J, Jevtovic-Todorovic V. The abolishment of anesthesia-induced cognitive impairment by timely protection of mitochondria in the developing rat brain: the importance of free oxygen radicals and mitochondrial integrity. Neurobiology of disease. 2012; 45:1031–41. [PubMed: 22198380]

27. Crompton M. The mitochondrial permeability transition pore and its role in cell death. The Biochemical journal. 1999; 341(Pt 2):233–49. [PubMed: 10393078]

28. Halestrap AP. What is the mitochondrial permeability transition pore? Journal of molecular and cellular cardiology. 2009; 46:821–31. [PubMed: 19265700]

29. Lamarche F, Carcenac C, Gonthier B, Cottet-Rousselle C, Chauvin C, Barret L, Leverve X, Savasta M, Fontaine E. Mitochondrial permeability transition pore inhibitors prevent ethanol-induced neuronal death in mice. Chemical research in toxicology. 2013; 26:78–88. [PubMed: 23268549]

30. Bai X, Yan Y, Canfield S, Muravyeva MY, Kikuchi C, Zaja I, Corbett JA, Bosnjak ZJ. Ketamine enhances human neural stem cell proliferation and induces neuronal apoptosis via reactive oxygen species-mediated mitochondrial pathway. Anesthesia and analgesia. 2013; 116:869–80. [PubMed: 23460563]

31. Bosnjak ZJ, Yan Y, Canfield S, Muravyeva MY, Kikuchi C, Wells CW, Corbett JA, Bai X. Ketamine induces toxicity in human neurons differentiated from embryonic stem cells via mitochondrial apoptosis pathway. Current drug safety. 2012; 7:106–19. [PubMed: 22873495]

32. Twaroski DM, Yan Y, Olson JM, Bosnjak ZJ, Bai X. Down-regulation of MicroRNA-21 Is Involved in the Propofol-induced Neurotoxicity Observed in Human Stem Cell-derived Neurons. Anesthesiology. 2014; 121:786–800. [PubMed: 24950164]

33. Ludbrook GL, Visco E, Lam AM. Propofol: relation between brain concentrations, electroencephalogram, middle cerebral artery blood flow velocity, and cerebral oxygen extraction during induction of anesthesia. Anesthesiology. 2002; 97:1363–70. [PubMed: 12459660]

34. Vutskits L, Gascon E, Tassonyi E, Kiss JZ. Clinically relevant concentrations of propofol but not midazolam alter in vitro dendritic development of isolated gamma-aminobutyric acid-positive interneurons. Anesthesiology. 2005; 102:970–6. [PubMed: 15851884]

35. Hilton GD, Stoica BA, Byrnes KR, Faden AI. Roscovitine reduces neuronal loss, glial activation, and neurologic deficits after brain trauma. Journal of cerebral blood flow and metabolism : official journal of the International Society of Cerebral Blood Flow and Metabolism. 2008; 28:1845–59.

36. Verdaguer E, Jorda EG, Canudas AM, Jimenez A, Pubill D, Escubedo E, Camarasa J, Pallas M, Camins A. Antiapoptotic effects of roscovitine in cerebellar granule cells deprived of serum and potassium: a cell cycle-related mechanism. Neurochemistry international. 2004; 44:251–61. [PubMed: 14602088]

37. Wu J, Kharebava G, Piao C, Stoica BA, Dinizo M, Sabirzhanov B, Hanscom M, Guanciale K, Faden AI. Inhibition of E2F1/CDK1 pathway attenuates neuronal apoptosis in vitro and confers neuroprotection after spinal cord injury in vivo. PloS one. 2012; 7:e42129. [PubMed: 22848730]

38. Benitez-King G, Ramirez-Rodriguez G, Ortiz L, Meza I. The neuronal cytoskeleton as a potential therapeutical target in neurodegenerative diseases and schizophrenia. Current drug targets CNS and neurological disorders. 2004; 3:515–33. [PubMed: 15581421]

39. Oyedele OO, Kramer B. Nuanced but significant: how ethanol perturbs avian cranial neural crest cell actin cytoskeleton, migration and proliferation. Alcohol. 2013; 47:417–26. [PubMed: 23731693]

40. Yamazaki Y, Tsuruga M, Zhou D, Fujita Y, Shang X, Dang Y, Kawasaki K, Oka S. Cytoskeletal disruption accelerates caspase-3 activation and alters the intracellular membrane reorganization in DNA damage-induced apoptosis. Experimental cell research. 2000; 259:64–78. [PubMed: 10942579]

41. Marsboom G, Toth PT, Ryan JJ, Hong Z, Wu X, Fang YH, Thenappan T, Piao L, Zhang HJ, Pogoriler J, Chen Y, Morrow E, Weir EK, Rehman J, Archer SL. Dynamin-related protein 1-mediated mitochondrial mitotic fission permits hyperproliferation of vascular smooth muscle cells and offers a novel therapeutic target in pulmonary hypertension. Circulation research. 2012; 110:1484–97. [PubMed: 22511751]

42. Gottlieb E, Armour SM, Harris MH, Thompson CB. Mitochondrial membrane potential regulates matrix configuration and cytochrome c release during apoptosis. Cell death and differentiation. 2003; 10:709–17. [PubMed: 12761579]

43. Dobbing J, Sands J. Comparative aspects of the brain growth spurt. Early human development. 1979; 3:79–83. [PubMed: 118862]

44. Orrenius S, Zhivotovsky B, Nicotera P. Regulation of cell death: The calcium-apoptosis link. Nat Rev Mol Cell Bio. 2003; 4:552–65. [PubMed: 12838338]

45. Cui Y, Ling-Shan G, Yi L, Xing-Qi W, Xue-Mei Z, Xiao-Xing Y. Repeated administration of propofol upregulated the expression of c-Fos and cleaved-caspase-3 proteins in the developing mouse brain. Indian journal of pharmacology. 2011; 43:648–51. [PubMed: 22144767]

46. Cao SE, Tian J, Chen S, Zhang X, Zhang Y. Role of miR-34c in ketamine-induced neurotoxicity in neonatal mice hippocampus. Cell biology international. 2015; 39:164–8. [PubMed: 25052764]

47. Wang Z, Jiang H, Chen S, Du F, Wang X. The mitochondrial phosphatase PGAM5 functions at the convergence point of multiple necrotic death pathways. Cell. 2012; 148:228–43. [PubMed: 22265414]

48. Frank S, Gaume B, Bergmann-Leitner ES, Leitner WW, Robert EG, Catez F, Smith CL, Youle RJ. The role of dynamin-related protein 1, a mediator of mitochondrial fission, in apoptosis. Developmental cell. 2001; 1:515–25. [PubMed: 11703942]

49. Grohm J, Kim SW, Mamrak U, Tobaben S, Cassidy-Stone A, Nunnari J, Plesnila N, Culmsee C. Inhibition of Drp1 provides neuroprotection in vitro and in vivo. Cell death and differentiation. 2012; 19:1446–58. [PubMed: 22388349]

50. Szabadkai G, Simoni AM, Chami M, Wieckowski MR, Youle RJ, Rizzuto R. Drp-1-dependent division of the mitochondrial network blocks intraorganellar Ca2+ waves and protects against Ca2+-mediated apoptosis. Molecular cell. 2004; 16:59–68. [PubMed: 15469822]

51. Martorell-Riera A, Segarra-Mondejar M, Munoz JP, Ginet V, Olloquequi J, Perez-Clausell J, Palacin M, Reina M, Puyal J, Zorzano A, Soriano FX. Mfn2 downregulation in excitotoxicity causes mitochondrial dysfunction and delayed neuronal death. The EMBO journal. 2014; 33:2388–407. [PubMed: 25147362]

52. Taguchi N, Ishihara N, Jofuku A, Oka T, Mihara K. Mitotic phosphorylation of dynamin-related GTPase Drp1 participates in mitochondrial fission. The Journal of biological chemistry. 2007; 282:11521–9. [PubMed: 17301055]

53. Zaja I, Bai X, Liu Y, Kikuchi C, Dosenovic S, Yan Y, Canfield SG, Bosnjak ZJ. Cdk1, PKCdelta and calcineurin-mediated Drp1 pathway contributes to mitochondrial fission-induced cardiomyocyte death. Biochem Biophys Res Commun. 2014; 453:710–21. [PubMed: 25445585]

54. Gomes LC, Scorrano L. Mitochondrial morphology in mitophagy and macroautophagy. Biochimica et biophysica acta. 2013; 1833:205–12. [PubMed: 22406072]

55. Kubli DA, Gustafsson AB. Mitochondria and mitophagy: the yin and yang of cell death control. Circulation research. 2012; 111:1208–21. [PubMed: 23065344]

56. Ong SB, Hausenloy DJ. Mitochondrial morphology and cardiovascular disease. Cardiovascular research. 2010; 88:16–29. [PubMed: 20631158]

57. Lamarche F, Carcenac C, Gonthier B, Cottet-Rousselle C, Chauvin C, Barret L, Leverve X, Savasta M, Fontaine E. Mitochondrial Permeability Transition Pore Inhibitors Prevent Ethanol-Induced Neuronal Death in Mice. Chemical research in toxicology. 2013

58. Lian G, Sheen VL. Cytoskeletal proteins in cortical development and disease: actin associated proteins in periventricular heterotopia. Frontiers in cellular neuroscience. 2015; 9:99. [PubMed: 25883548]

59. Bellenchi GC, Gurniak CB, Perlas E, Middei S, Ammassari-Teule M, Witke W. N-cofilin is associated with neuronal migration disorders and cell cycle control in the cerebral cortex. Genes & development. 2007; 21:2347–57. [PubMed: 17875668]

60. Riu PL, Riu G, Testa C, Mulas M, Caria MA, Mameli S, Mameli O. Disposition of propofol between red blood cells, plasma, brain and cerebrospinal fluid in rabbits. European journal of anaesthesiology. 2000; 17:18–22. [PubMed: 10758439]
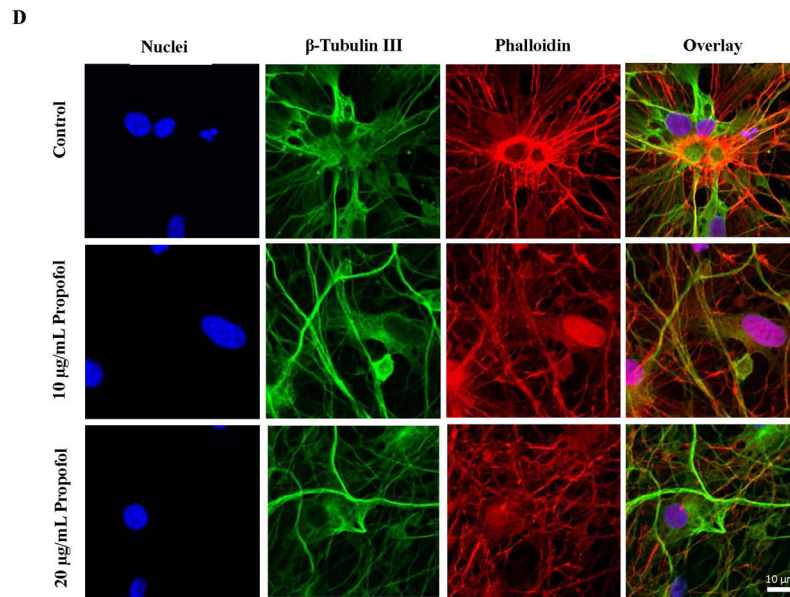
A

β-Tubulin III
Nuclei

Doublecortin
Nuclei

Overlay
Nuclei

B

C
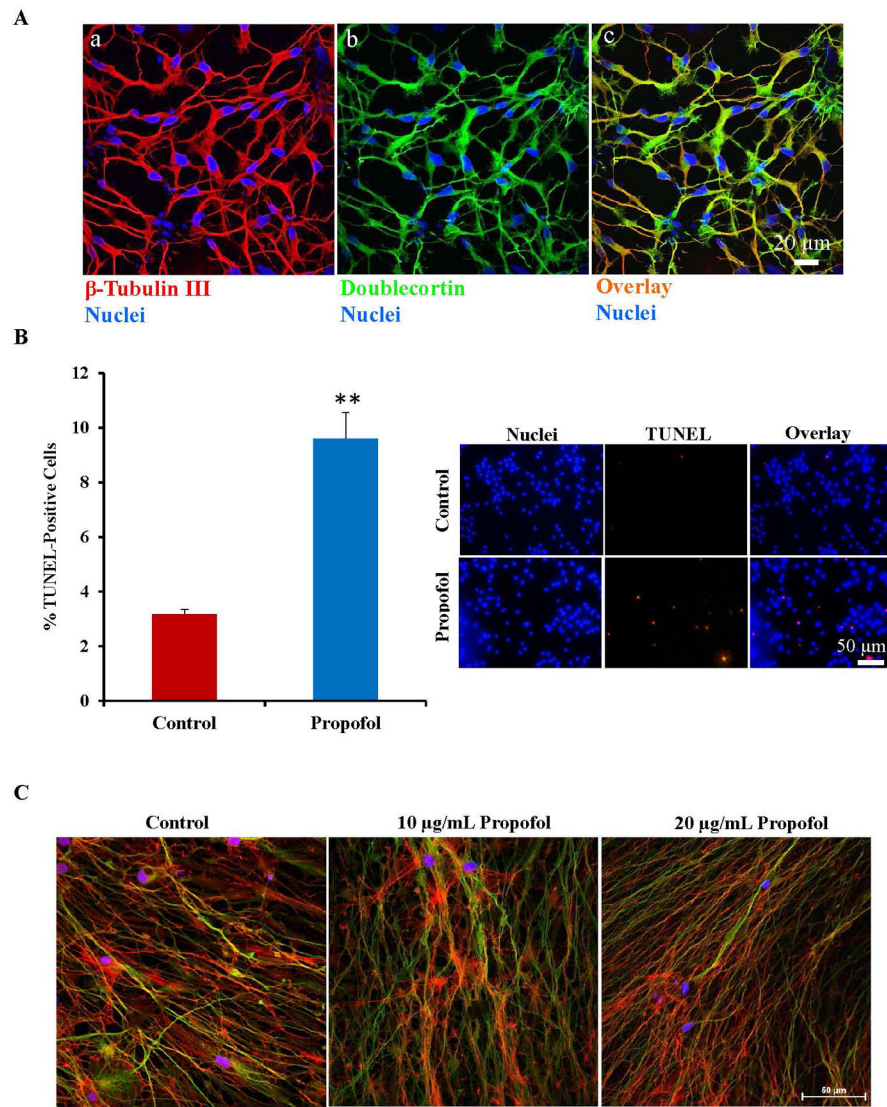
Fig. 1.

Human embryonic stem cell (hESC)-derived neurons were characterized by immunofluorescence staining and exposure of the neurons to propofol induced a significant increase in cell death and cytoskeletal disorganization. *(A)* Over 90–95% of the differentiated cells stained positive for the neuron specific marker, β-tubulin III (a) and the immature neuronal marker, doublecortin (b). The β-tubulin III and doublecortin staining co-localized which can be seen in orange in the overlay image (c). The cell nuclei were stained with Hoechst 33342 and are the blue dots in each image. *(B)* TUNEL staining was used to assess cell death in hESC-derived neurons exposed to propofol or the vehicle, DMSO. The number of TUNEL-positive cells (red dots) was manually counted along with the total nuclei present in the field (blue dots stained with Hoechst 33342). The percent of TUNEL positive cells was then calculated. Exposure of hESC-derived neurons to 20 μg/mL propofol for 6 hours induced a significant increase in the number of TUNEL-positive cells, indicating an increase in cell death. *(C)* Following exposure to 6 hours of the vehicle-control, DMSO or 10 μg/mL or 20 μg/mL propofol, the cells were also co-stained for Phalloidin, an F-actin marker and β-tubulin III. Nearly all of the cells in culture stained positive for β-tubulin III in all groups, indicating high differentiation efficiency. *(D)* Exposure to 10 μg/mL propofol induced disorganization of the actin cytoskeleton when compared to control-treated neurons. Further cytoskeletal disorganization was observed in the 20 μg/mL propofol treated group. (**$P < 0.01$ vs. Control, n = 5/group). TUNEL = terminal deoxynucleotidyl transferase-mediated deoxyuridine triphosphate in situ nick end labeling. DMSO = dimethyl sulfoxide.
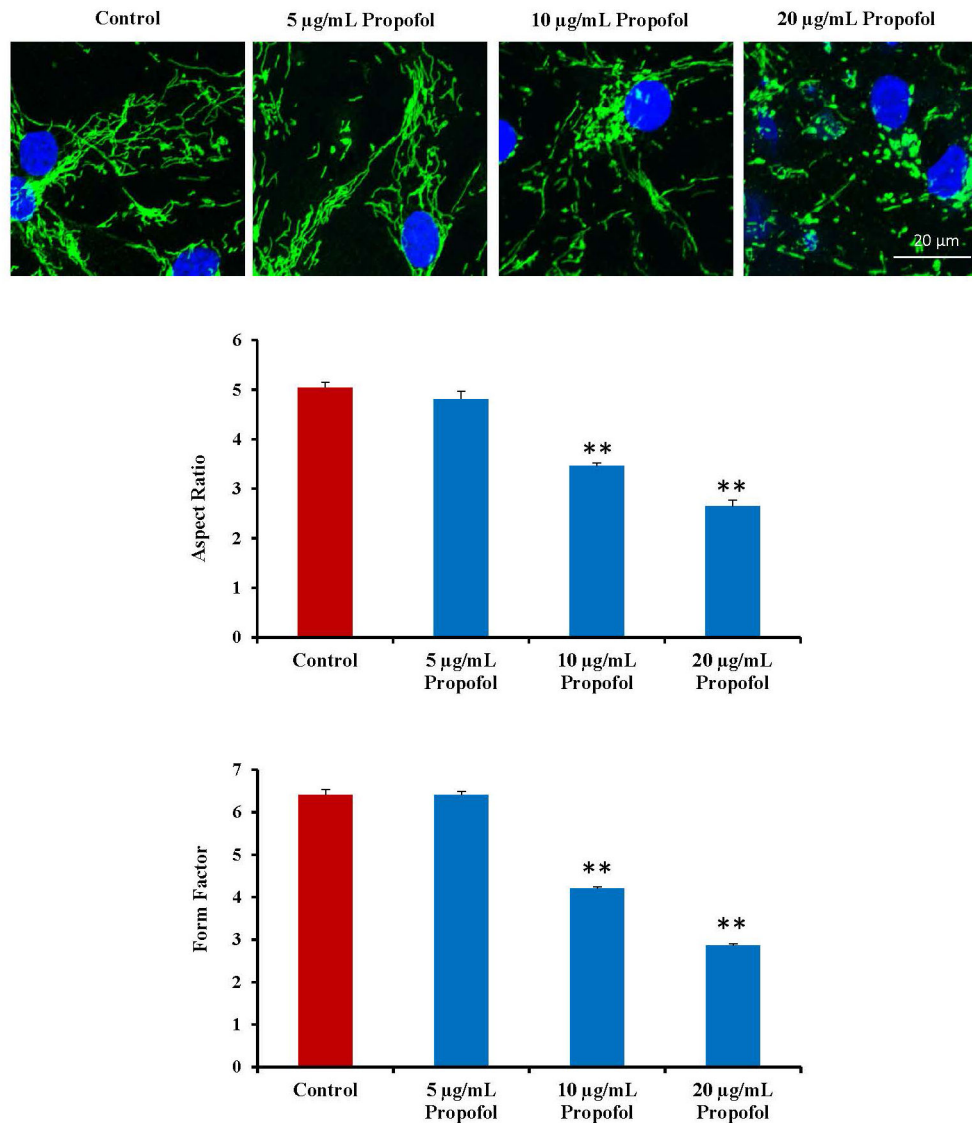
Fig. 2.
Propofol dose-dependently induces mitochondrial fission in human embryonic stem cell (hESC)-derived neurons. hESC-derived neurons were exposed for 6 hours to dimethyl sulfoxide (DMSO) as the vehicle control or 5, 10 or 20 µg/mL propofol. The cells were then immunostained using a mitochondrial antibody to visualize the mitochondria. The mitochondrial morphology was assessed by imaging the cells on the confocal microscope. The mitochondria appeared elongated and interconnected in the control and 5 µg/mL propofol-treated groups. The mitochondria became significantly fragmented following exposure to 10 µg/mL propofol with further fragmentation observed in the 20 µg/mL propofol-treated group. The form factor (FF, mitochondrial branching) and the aspect ratio (AR, mitochondrial length) were analyzed using the ImageJ software. Both factors were significantly reduced in the 10 and 20 µg/mL propofol-treated groups, confirming mitochondrial fission in these groups. (**$P < 0.01$ vs. control, n = 5 coverslips/group).
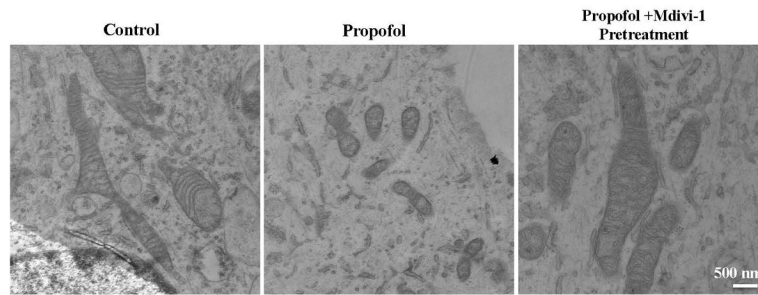
Figure 3A

Figure 3B

Control   **Propofol**   **Propofol +Mdivi-1 Pretreatment**
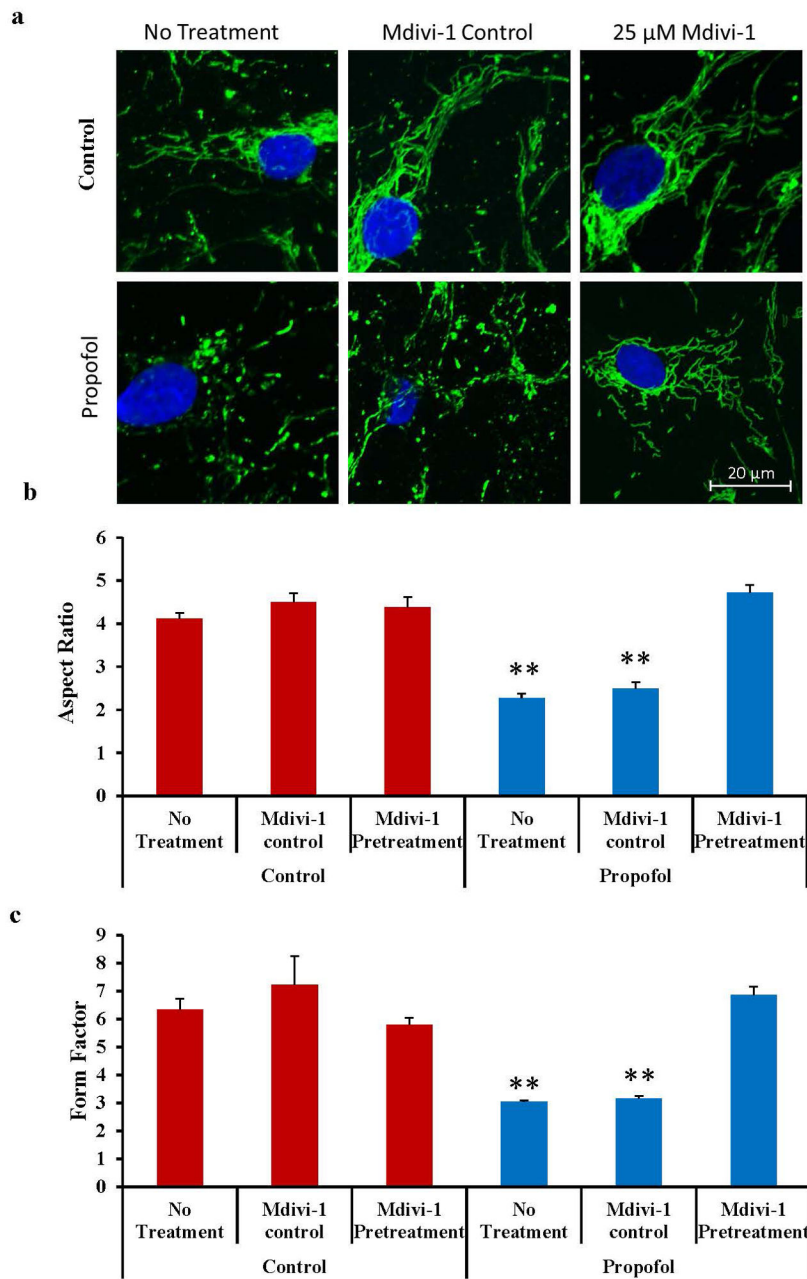
Fig. 3.

Propofol exposure induced severe mitochondrial fragmentation in human embryonic stem cell (hESC)-derived neurons. *(A)* hESC-derived neurons were exposed to 6 hours of 20 μg/mL propofol or the vehicle control and immunostaining with the TOM20 (translocase of outer mitochondrial membranes 20 kDa) antibody was used to visualize the mitochondria. The cells were then imaged on the confocal microscope to assess the mitochondrial morphology. The mitochondria appeared severely fragmented following propofol exposure and this was rescued by pretreatment of the cells for 1 hour with 25 μM mdivi-1 (a). The images were analyzed using ImageJ to assess the form factor (mitochondrial branching) and the aspect ratio (mitochondrial length). The aspect ratio was significantly reduced in the propofol-treated group indicating mitochondrial fragmentation. This was rescued by pretreatment of the cells for 1 hour with 25 μM mdivi-1 (b). The form factor was also significantly reduced in the cells treated with propofol alone or propofol with mdivi-1 control pretreatment when compared to all control-treated groups, further indicating increased mitochondrial fission. The form factor was rescued to control levels in cells pretreated for 1 hour with 25 μM mdivi-1 prior to propofol exposure (c). *(B)* hESC-derived neurons exposed to propofol or control conditions with or without mdivi-1 pretreatment were fixed and imaged using electron microscopy to visualize the cellular ultrastructure and mitochondrial morphology. The mitochondria of the control treated group were large and elongated with clear cristae and appeared generally healthy. In contrast, the mitochondria in the propofol-treated group were extremely small with disorganized and abnormal inner mitochondrial membranes. These mitochondrial abnormalities were not present in the propofol-treated group when the cells were pretreated with the mitochondrial fission blocker, mdivi-1. (**$P < 0.01$ vs. all control groups and propofol mdivi-1 pretreatment group, n = 5 coverslips/group).
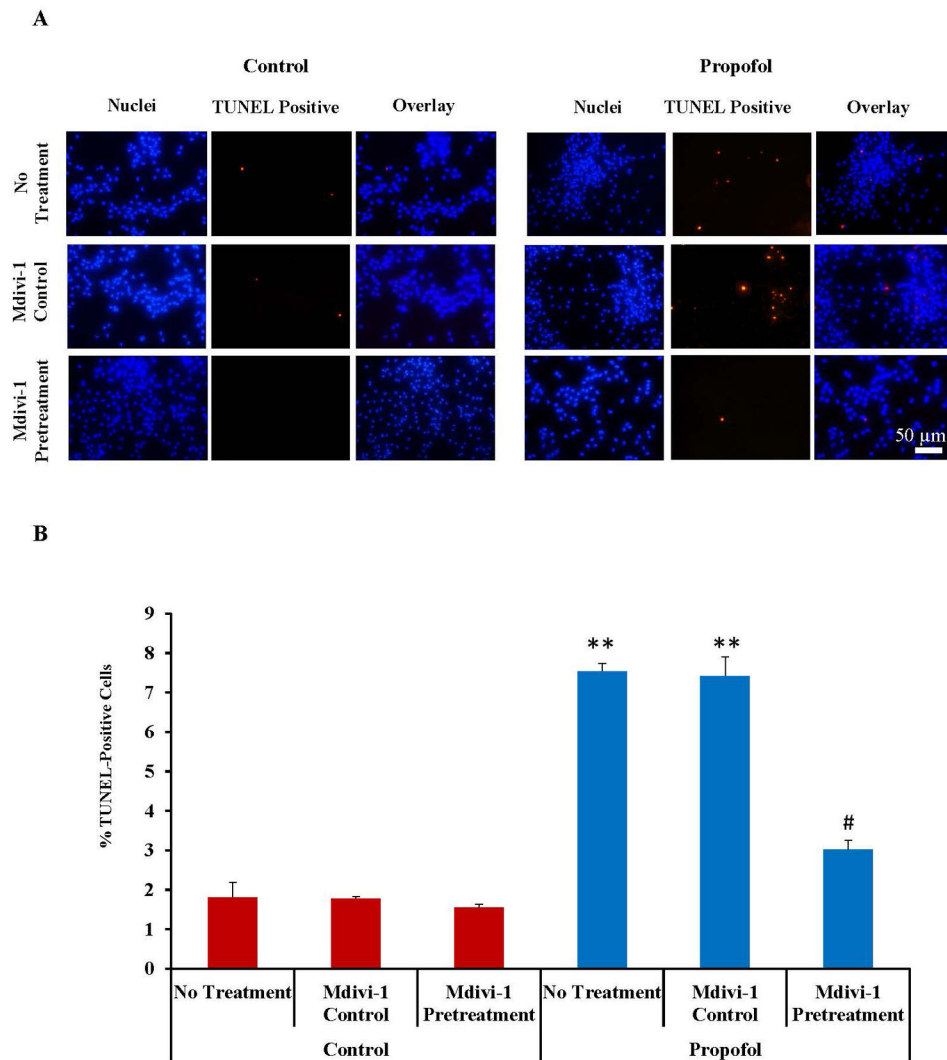
A

B

Fig. 4.

Propofol induced cell death was attenuated by pretreatment of the cells with the mitochondrial fission blocker, mdivi-1. *(A)* TUNEL staining was used to assess cell death in human embryonic stem cell (hESC)-derived neurons. Cells were exposed for 6 hours to 20 µg/mL propofol or the vehicle control following a 1 hour pretreatment with media alone (no treatment), the mdivi-1 vehicle control (mdivi-1 control) or 25 µM mdivi-1 (mdivi-1 pretreatment) and stained using the TUNEL kit. Most of the TUNEL staining (red dots) co-localized with the nuclei stain (blue dots stained with Hoechst 33342) and there were more TUNEL positive cells observed in the "propofol no treatment" and "propofol midivi-1 control" treated groups when compared to all other groups. *(B)* The number of TUNEL-positive cells and total cell nuclei present in the field were manually counted to obtain a percent of TUNEL-positive cells. The percent of TUNEL-positive cells was significantly increased in the "propofol no treatment" and "propofol mdivi-1 control" treated groups when compared to all control-treated groups indicating increased cell death. The increase in cell death was attenuated by mdivi-1 pretreatment. (**$P < 0.01$ vs. all control groups and propofol mdivi-1 pretreatment group, # $P < 0.01$ vs. dimethyl sulfoxide (DMSO). mdivi-1

pretreatment group, n = 5 coverslips/group). TUNEL = terminal deoxynucleotidyl transferase-mediated deoxyuridine triphosphate in situ nick end labeling.

A

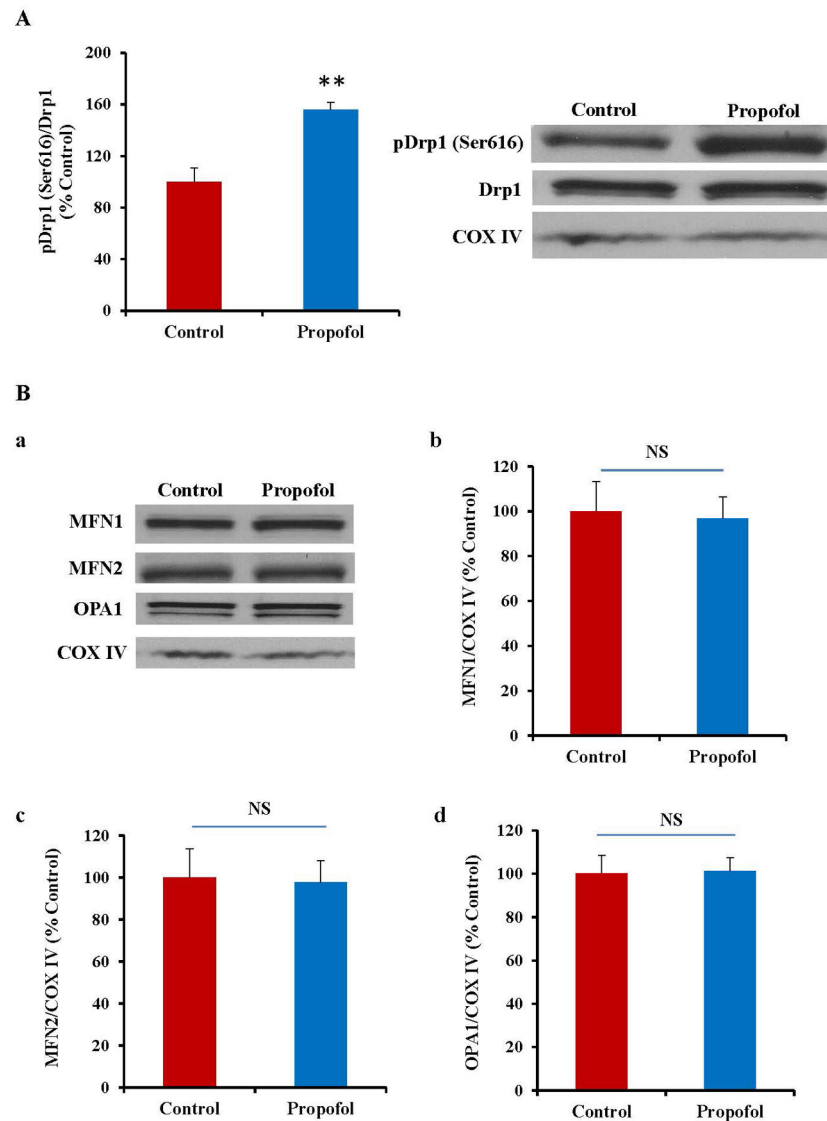
B

a

b

c

d

Fig. 5.

Exposure of human embryonic stem cell (hESC)-derived neurons to propofol altered the expression of the mitochondrial fission-related protein and did not affect mitochondrial fusion. *(A)* Western blotting was used to assess the expression of dynamin-related protein 1 (Drp1), a protein responsible for inducing mitochondrial fission. Drp1 becomes activated when phosphorylated at the Ser616 position. Exposure of hESC-derived neurons to 6 hours of 20 μg/mL propofol significantly increased the expression of activated Drp1 (pDrp1 Ser 616). The data are presented as a ratio of pDrp1/total Drp1 and as a percent of the control *(B)* Western blotting was also used to assess the expression of mitofusion 1 and 2 (MFN1 and MFN2) and optic atrophy 1 (OPA1), proteins all responsible for inducing mitochondrial fusion (a). Following 6 hours of exposure to 20 μg/mL propofol, there was no significant change in the expression of MFN1, MFN2 or OPA1 when compared to control treated cells (b–d), indicating that propofol exposure does not significantly affect mitochondrial fusion. These data are presented as a percent of the control group following normalization to COX

IV, a marker of the inner mitochondrial membrane. (**$P < 0.01$, n = 5/group). NS = Not significant.

A
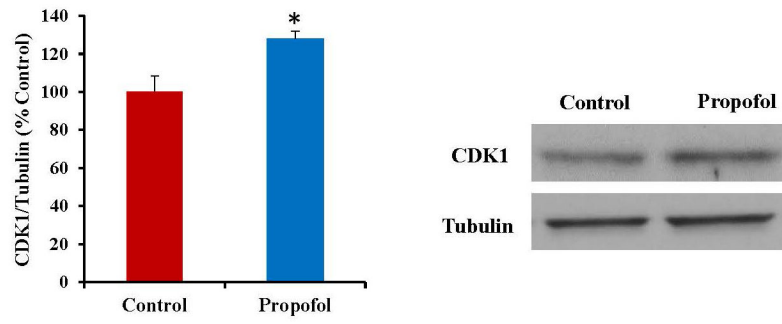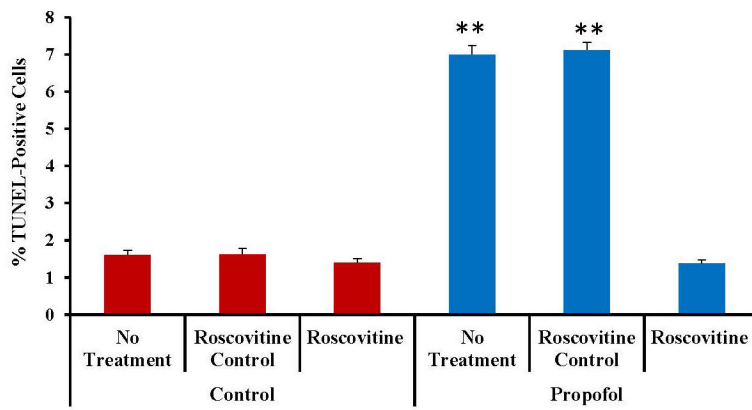
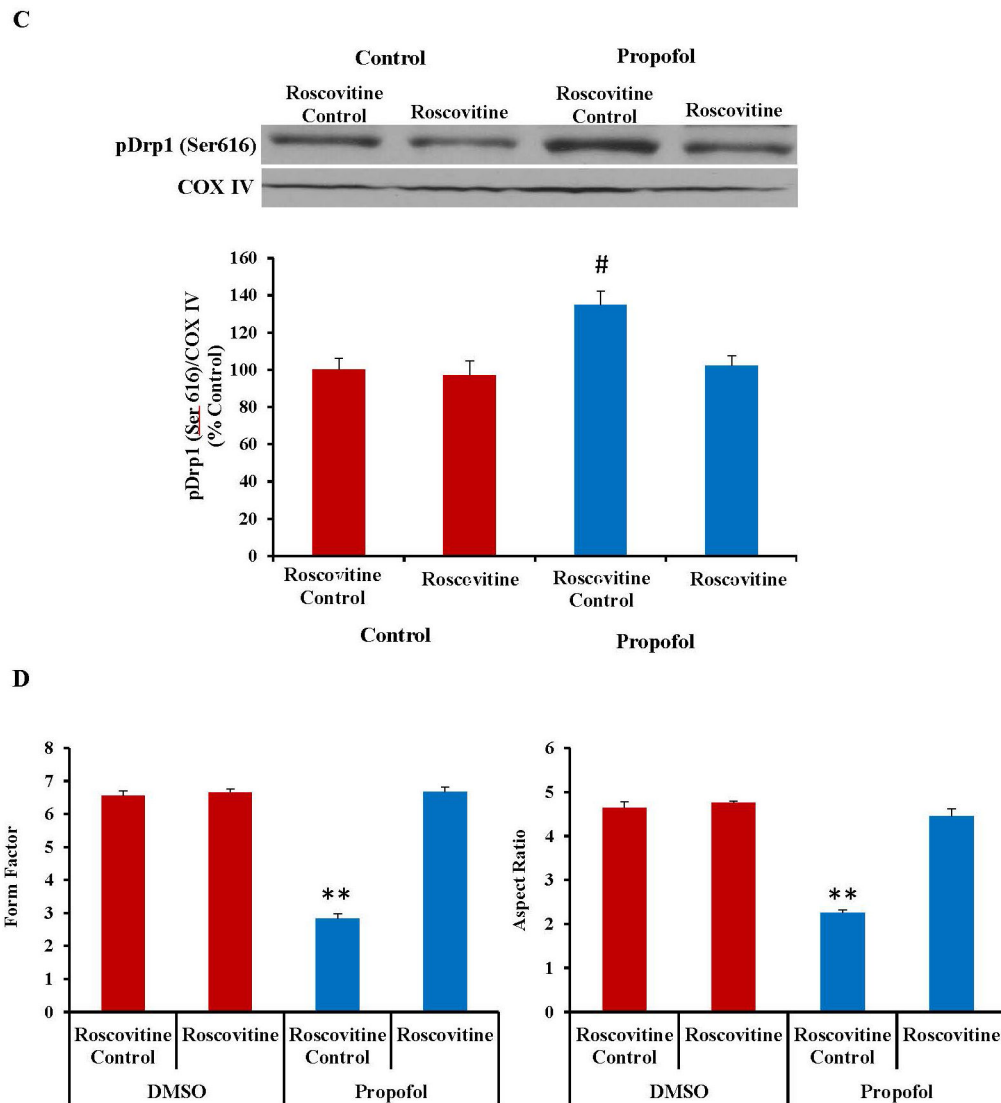

B

C

D

Fig. 6.

The expression of cyclin dependent kinase 1 (CDK1) was significantly increased in human embryonic stem cell (hESC)-derived neurons following exposure to propofol and inhibition of CDK1 attenuated the propofol-induced cell death, dynamin-related protein 1 (Drp1) activation and mitochondrial fission. *(A)* CDK1 is responsible for phosphorylating Drp1 at the serine 616 position which, in turn, activates Drp1 and induces mitochondrial fission. The expression of CDK1 was significantly increased following exposure to 6 hours of 20 μg/mL propofol when compared to control treated cells as assessed by Western blot. *(B)* Blockade of CDK1 by pretreatment of the cells with Roscovitine attenuated the propofol-induced cell death as assessed by TUNEL staining, indicating that CDK1 is involved in propofol-induced neurotoxicity. *(C)* Pretreatment of the cells with Roscovitine also attenuated the propofol-induced activation of Drp1 (pDrp1 Serine 616) as assessed by Western blot, further confirming the role of CDK1 and Drp1 in propofol-induced neuronal cell death. This data is presented as a percent of the control group following normalization to COX IV. *(D)* Finally,

pretreatment of the cells with Roscovitine attenuated the propofol-induced mitochondrial fission as assessed by immunostaining for the mitochondrial-specific marker, TOM20 (translocase of outer mitochondrial membranes, 20 kDa). This finding confirms the role of CDK1 in propofol-induced mitochondrial fission. (*$P < 0.05$ vs. control, **$P < 0.01$ vs. all other groups, #$P < 0.05$ vs. all other groups, n = 5/group). TUNEL = terminal deoxynucleotidyl transferase-mediated deoxyuridine triphosphate in situ nick end labeling. DMSO = dimethyl sulfoxide (the vehicle control).
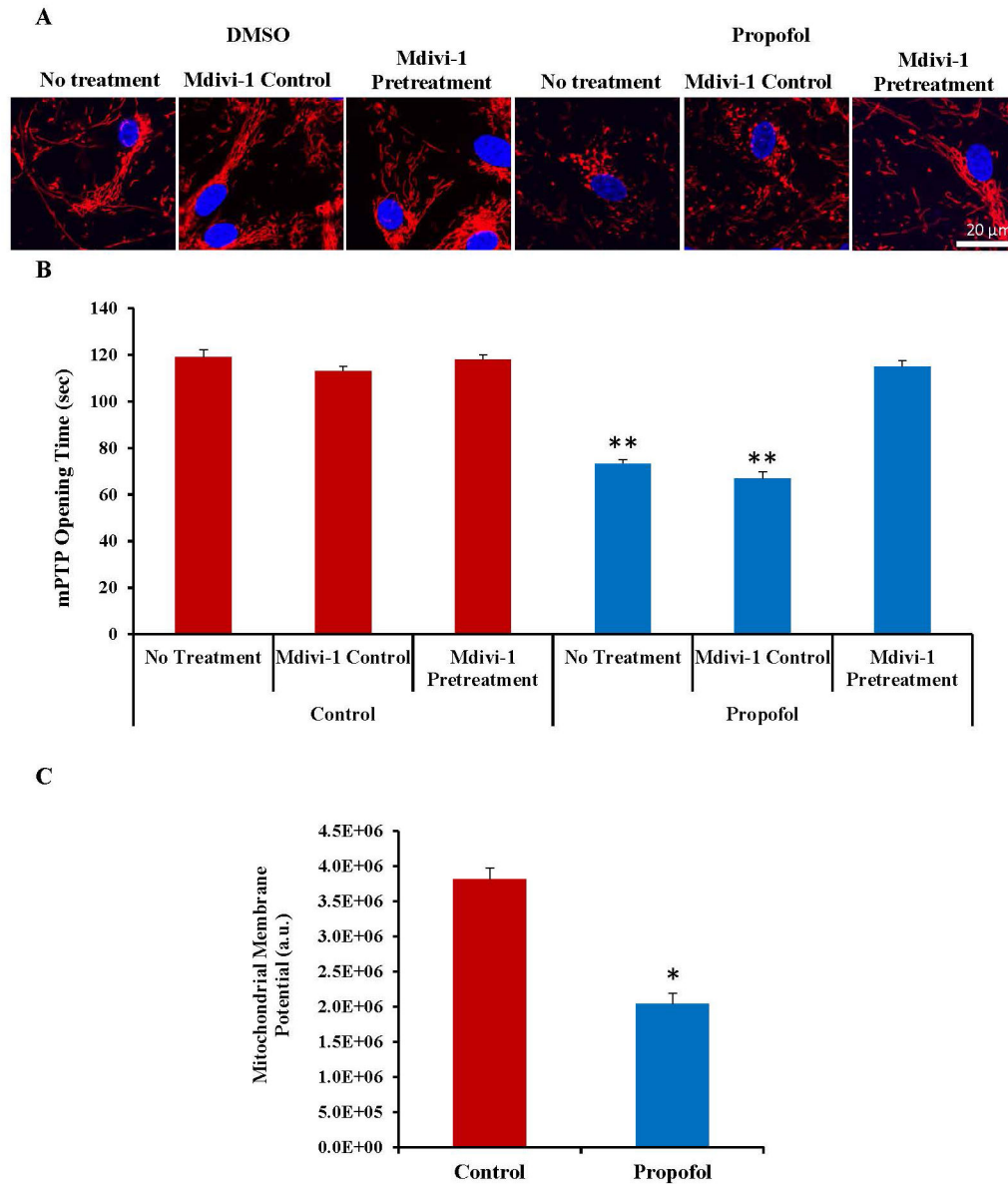
Fig. 7.

Propofol reduced the mitochondrial membrane potential and induced an earlier opening of the mitochondrial permeability transition pore (mPTP) in human embryonic stem cell (hESC)-derived neurons and mPTP opening was delayed by blockade of mitochondrial fission. hESC-derived neurons were exposed for 6 hours to 20 μg/mL propofol or control with or without mdivi-1 pretreatment and loaded for 20 minutes with 50 nM tetramethylrhodamine ethyl ester (TMRE), a red dye taken up by the mitochondria. Rapid laser scanning (imaging the cells every 3.5 seconds for 55 frames) using the 561 nm laser of the confocal microscope was used to generate oxidative stress and induce opening of the mPTP. *(A)* The mitochondria appeared severely fragmented in the "propofol no treatment" and "propofol mdivi-1 control" groups. *(B)* Opening of the mPTP was observed as a rapid loss of TMRE fluorescence which was traced by plotting the fluorescence intensity recorded

at each of the 55 frames obtained during the photoexcitiation. Arbitrary mPTP opening time was assessed by determining the time at which TMRE fluorescence had decreased by half between the initial and residual TMRE fluorescence. Propofol exposure induced a significantly earlier opening of the mPTP which was rescued to control levels by pretreatment for 1 hour with 25 μM mdivi-1. *(C)* The mitochondrial membrane potential was also assessed in the cells following exposure to the vehicle control or propofol by loading the cells with TMRE and imaging on the confocal microscope. Propofol exposure reduced the mitochondrial membrane potential in the cells when compared to control-treated cells further indicating mitochondrial damage following propofol exposure. (**$P < 0.01$ vs. all control groups and propofol mdivi-1 pretreatment group, *$P < 0.05$ vs. control, n = 5 coverslips/group). DMSO = dimethyl sulfoxide (the vehicle control).